Review Article

Journal of Textile Engineering and Fashion Technology

Application of Warp Knit Spacer Fabrics in Tissue Engineering

N Gokarneshan*, Neeti Kishore, PG Anandhakrishnan, S Sumitha, R Sasirekha, Obulam Vidya Sagar, Subhani Sharma, Navya Sudheer, R Haritha and Andrea Samuels

Department of Fashion Design and Arts, Hindustan Institute of Technology and Science, Chennai, India

***Corresponding author**
N Gokarneshan, Department of Fashion Design and Arts, Hindustan Institute of Technology and Science, Chennai, India

Submitted: 19 Nov 2021; **Accepted:** 25 Nov 2021; **Published:** 01 Dec 2021

Citation: *N Gokarneshan, Neeti Kishore, PG Anandhakrishnan, S Sumitha, R Sasirekha, Obulam Vidya Sagar, Subhani Sharma, Navya Sudheer, R Haritha and Andrea Samuels. (2021). Application of Warp Knit Spacer Fabrics in Tissue Engineering. 3(1), 44-49.*

Abstract

Mesenchymal stem cells (MSCs) possess huge potential for regenerative medicine. For tissue engineering approaches, sca_olds and hydrogels are routinely used as extracellular matrix (ECM) carriers. The present study investigated the feasibility of using textile-reinforced hydrogels with adjustable porosity and elasticity as a versatile platform for soft tissue engineering. A warp-knitted poly (ethylene terephthalate) (PET) sca_old was developed and characterized with respect to morphology, porosity, and mechanics. The textile carrier was infiltrated with hydrogels and cells resulting in a fiber-reinforced matrix with adjustable biological as well as mechanical cues. Finally, the potential of this platform technology for regenerative medicine was tested on the example of fat tissue engineering. MSCs were seeded on the construct and exposed to adipogenic differentiation medium. Cell invasion was detected by two-photon microscopy, proliferation was measured by the PrestoBlue assay. Successful adipogenesis was demonstrated using Oil Red O staining as well as measurement of secreted adipokines. In conclusion, the given microenvironment featured optimal mechanical as well as biological properties for proliferation and di_erentiation of MSCs. Besides fat tissue, the textile-reinforced hydrogel system with adjustable mechanics could be a promising platform for future fabrication of versatile soft tissues, such as cartilage, tendon, or muscle.

Key words: Tissue Engineering, Biofabrication, Biohybrid Sca_Old, Textile Engineering

Introduction

Mesenchymal stem cells (MSCs) are multipotent progenitor cells in the stroma of several tissues in the body, which can di_erentiate in several cell types of the mesodermal lineage, i.e., adipocytes, osteoblasts, chondrocytes, and myocytes [1]. They have been defined by the Committee of the International Society for Cellular Therapy by their ability to di_erentiate and by being plastic adherent in standard culture conditions [2]. MSCs can be obtained from various tissues, especially bone marrow and adipose, and are used as cell sources for therapeutic or experimental exploitation [3]. Adipose tissue is a composition of regenerative cell types containing not only adipocytes, but also MSCs, including adipose-derived stromal cells, and preadipocytes [4,5]. It is nowadays one of the most relevant cell sources, because adipose tissue contains approximately 500 times more MSCs compared to bone marrow [5]. In addition, adipose tissue can be harvested more easily and less invasive than bone marrow, e.g., by liposuction [4].

For the above-mentioned reasons, adipose tissue-derived stromal cells are of great interest in the field of regenerative medicine and tissue engineering and over an ideal cell source for the treatment of large size soft tissue defects. The current gold standard for treating such defects, e.g., breast reconstruction after mastectomy or defects after trauma, is the transplantation of autologous tissue, which is always associated with a second operation field and the risk of donor site morbidity [6 -8]. Thus, several approaches target at the generation and transplantation of artificial tissue to repair damaged or replace lost tissue. As a growth matrix, biomaterial-derived sca_olds are widely used in tissue engineering, in both in vitro and in vivo experiments [9,10]. Besides rigid metal, polymer, or ceramic sca_olds, hydrogels gained special attraction as matrix material for soft tissue regeneration [11-13].

They provide a good environment for three-dimensional cell culture due to their high water content, their ECM-like structure, and the presence of cell adhesion motifs [14,15]. Numerous studies have described the biochemical and biophysical properties of hydrogels and their excellent ability to mimic the cell physiological microenvironment [16]. In particular, the e_ect of spatiotemporal modulated mechanics on stem cell fate is in the focus of attention [17]. However, hydrogels lack mechanical strength and stability. For this reason, their clinical applicability is very limited. Mechanical strength and stiffness are not only of importance in load-bearing implants, such as bone or cartilage, but also play a major role in soft tissue mechanics. For instance, to enable safe scaffold handling and suture retention during surgery,

even hydrogel -cell constructs for soft tissue repair must withstand mechanical stress.

To overcome the shortcoming of poor mechanical properties, while maintaining their elastic nature, hydrogels can be reinforced with textile structures. The basic stability of the adipose tissue is given by the superficial fascia system contained therein. This fascia layer ensures stability and displacement of the soft tissue. It also provides skin attachment to underlying structures. Thus, stability through body fascia in the apparently unstable adipose tissue is highly relevant.

Up to now, successful textile reinforcement could be shown for thin, planar, and cylindricalstructures, such as heart valves or blood vessels [18,19], using 2D textile meshes. The goal of the current study is to investigate the potential of 3D textile morphologies as building block for the generation of thick soft tissue structures. In particular, the mechanical and biological properties of warp-knitted spacer fabrics and their applicability as adipose cell matrix will be elucidated in the present study (Scheme 1). Due to their well-adjustable porosity, pore size, and Young's modulus, we consider spacer fabrics an extremely versatile scaffold not limited to fat tissue applications but also suitable for a broad range of soft and hard tissues, such as bone, cartilage, and muscle.

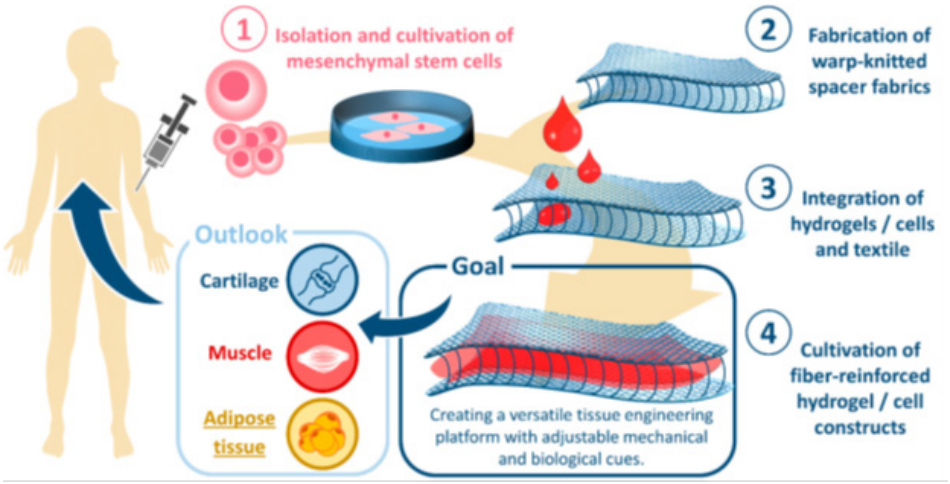

Biofabrication of Textile-Reinforced Hydrogels Scaffolds

The present study describes a novel approach to generate fiber-reinforced hydrogel sca_olds for tissue engineering applications. PET spacer fabrics were produced using warp-knitting technology. These scaffolds were further combined with polysaccharide- and protein-based hydrogels as well as living cells. The morphology and mechanics of these hybrid sca_olds were studied together with their cell biological response. Spacer fabrics are three-dimensional textile sca_olds that comprise an upper and lower cover area connected with multiple pile yarns (Figure 1A). Depending on the machine settings different pile yarn Materials 2020, 13, 3518 8 of 16

geometries can be applied (Figure 1B). For the cover areas, a broad range of designs and morphologies can be selected from (Figure 1C) pile yarn geometries can be applied (Figure 1B). For the cover areas, a broad range of designs and morphologies can be selected from (Figure 1C).

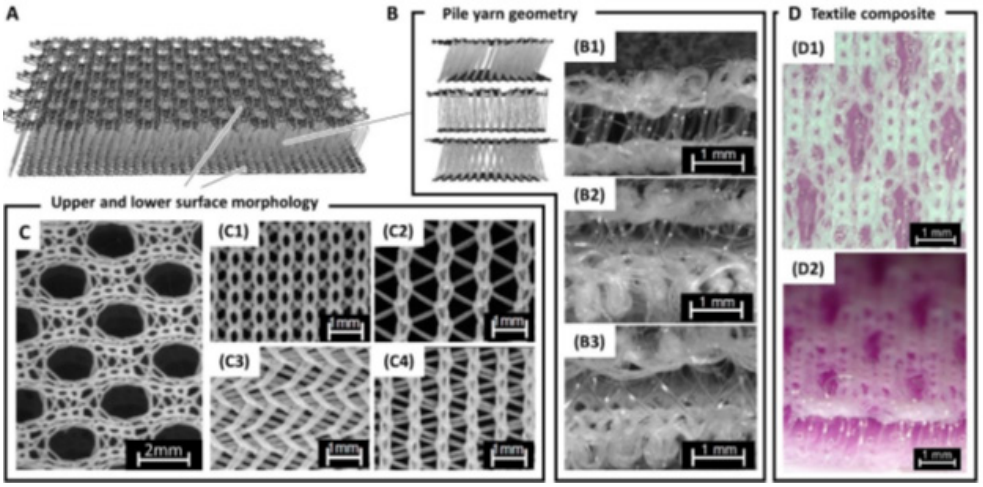

Following the fabrication process, the spacer fabrics were cut into circular samples with diameters 5, 15, and 26 mm using a laser cutter (Figure 2). During laser cutting, di_erent e_ects concerning the cutting quality could be observed (Figure 2B). Due to heat generation, parts of the cover areas and pile yarns melted hampering the separation of the samples. In addition, the melted material could result in partially occlusion of the open porous sca_olds geometry. Under optimal conditions clearly cut samples with an open, non-glued pile yarn geometry could be produced (Figure 2C).

The morphology, in particular the thickness, pore size, and porosity, of the fabricated sca_olds was analyzed using -CT imaging. The warp-knitted spacer fabrics had a thickness of 1.56 _ 0.06 mm, with a pile yarn height of 1.03 _ 0.09 mm. Porosity and pore size are important features for a tissue engineering scaffold as they might impact cell attachment, cell proliferation, as well as nutrient diffusion and removal of metabolic substances. The porosity (F) of the produced spacer fabrics was measured to be 43.4% _ 1.45% (Figure 3A). The pore size distribution peaked at ~560 _m and had an additional local maximum at ~120 _m. In more detail, 12.5% of the pores were below 200 _m, the majority (51.4%) were in the range of 200 to 500 _m, and 36.1% were bigger than 500 _m.

The morphology, in particular the thickness, of the fabricated scaffolds was analyzed using µ-CT imaging. The warp-knitted spacer fabrics had a thickness of 1.56 ± with a pile yarn height of 1.03 ± 0.09 mm. important a tissue engineering scaffold as they might impact cell attachment, cell proliferation, as well as nutrient diffusion and removal of metabolic substances. The porosity (Φ) of the produced spacer fabrics was measured to be 43.4% ± 1.45% (Figure 3A). The pore size distribution peaked at ~560 µm and had an additional local maximum at ~120µm. In more detail, 12.5% of the pores were below 200 µm, the majority (51.4%) were in the range of 200 to 500 µm, and 36.1% were bigger Next, the spacer fabric's mechanical properties were assessed. The spacer fabric's tensile properties were tested in a uniaxial as well as a biaxial experimental set-up. In the uniaxial tensile test, the scaffolds withstood an averaged maximum tensile force of 607.284 _ 19.52 N before break and exhibited a respective tensile Young's modulus of 6.74 MPa. In the biaxial testing, the bare textile scaffold was measured and compared with hydrogel filled composites. In contrast to the conventional uniaxial testing, the results are given as the measured slope of the force/strain curve. For each measurement, the samples were tested in 5 iterative stress/strain and relaxation cycles. During the repetitive measurement, it could be observed that the slope of the curve increased with every cycle (start, middle, end of the cycles), which can be contributed to a variation in the textile's structural elasticity. The same effect could be detected for the hydrogel filled spacer fabrics. Interestingly, the agarose filled textile exhibited a significantly lower slope compared to the bare textile and the textile-reinforced agarose -collagen and collagen sample.

To determine the rheological behavior of the applied hydrogels a viscosity measurement was conducted. For agarose, the zero shear viscosity was determined to be 30 mPa.s. The first Newtonian plateau was reached at a shear rate of 1.76. The zero-shear viscosity of the agarose -collagen blend was measured to be 86 mPa.s. For agarose -collagen, the first Newtonian plateau was detected at a shear rate of 1.74 s. The rheological measurements of collagen showed no clear first Newtonian plateau. Furthermore, the flow consistency index k and the flow behavior index n, applied in power-law modeling of the fluids, were calculated. The measurements resulted in flow consistency indices of 37 mPa.s for agarose, 105 mPa.s for agarose/collagen, and 69 mPa.s for collagen. The flow behavior index was measured to be 0.985 for agarose, 0.907 for agarose/collagen, and 1.03 for collagen.

Finally, the compressive Young's modulus of the applied hydrogels, the textile sca_olds, and the textile reinforced hydrogels was measured. The non-reinforced hydrogels exhibited rather low young's moduli ranging from 0.4 kPa (collagen) to 4.5 kPa (agarose -collagen) and 7.4 kPa (agarose). The textile scaffold showed a significantly increased compressive sti_ness (21.8 kPa). Interestingly, the three textile reinforced hydrogels exhibited the highest moduli ranging from 45.3 to 57.6 kPa.

Cellular Viability

Cellular viability was assessed by the Presto Blue (PB) assay for investigation of the cells' metabolic activity, as well as by crystal violet staining for evaluation of the final cell amount at the end of the experiment. The vitality of MSCs was measured by the PB assay and served as indicator for cellular proliferation over the course of the complete experiment [20]. After seeding the cells onto the knitted fabric, the cells attached to the fiber surface and were found equally distributed inside the scaffold. The initial PB conversion of 100,000 -400,000 cells was all on similar levels. This suggests that in these approaches the same amount of cells adhered to the scaffold. Seeding 50,000 cells in a smaller volume of cell suspension reduced the PB data at Day 0. On the following days of measurements, the metabolic activity of all cell numbers increased in a comparable manner reaching similar levels beginning with Day 14, followed by a parallel development until the end of the experiment. Two-way ANOVA with repeated measures after Greenhouse -Geisser correction determined significant differences between the days ($F_{days}(2.544, 91.587) = 461.38$, $p < 0.001$), between the cell numbers ($F_{cell\ numbers}(3, 36) = 5.889$, $p = 0.002$), and the interaction between both factors ($F_{days\ cell\ numbers}(7.632, 91.578) = 3.118$, $p = 0.004$). The following Bonferroni post hoc test found significant differences in metabolic activity on Day 0 between 50,000 cells and all other groups ($p < 0.001$), as well as between 50,000 and 100,000 cells at Day 7 ($p = 0.025$) (Figure 4B). After the final PB measurement on Day 28, the relative cell number was assessed by crystal violet staining in order to approve the PB data. Cell numbers were all on similar levels after 28 days of regular culture (Figure 4C). One-way ANOVA did not detect significant differences between the groups ($F(3, 36) = 1.677$, $p = 0.189$). For comparison, a 28-day 2-D culture of initially 100,000 MSC (n = 3) on a 12-well plate (surface area ~3.8 cm2) was stained with crystal violet, also (Figure 4C), which resulted in a staining level equal to the scaffold culture experiments. This suggests a comparable cell proliferation at both culture conditions.

Cell Differentiation

Adipogenic differentiation was induced by culturing MSCs for 10 days in differentiation medium

and assessed using Oil Red O staining as an indicator of intracellular lipid accumulation [21]. Lipid droplets were clearly stained in 2D culture (Figure 5A), whereas staining in the 3D cultures was hard to identify due to thickness and consistency of the fiber network. However, we found labeled cells also on the scaffold. For further detection of successful adipogenic differentiation, we measured the levels of two adipokines, which were exclusively released from adipocytes during development and maturity. Cell supernatants from untreated cells as well as 2D and 3D cultures exposed to differentiation medium were analyzed for their content of leptin and serpin. The latter was below detection level in the untreated control, while the basal leptin was at 2 pg/mL Adipogenic di_ erentiation of MSCs significantly increased the release of both cytokines. For serpin, the measures were on comparable levels (1.7 ng/mL), while in 3D culture di_erentiation of the leptin levels was significantly increased compared to the 2D condition.

Discussion

A novel approach for the biofabrication of fiber-reinforced hydrogels with adjustable morphological characteristics and mechanics is presented. Three-dimensional PET spacer fabrics were generated using warp-knitting technology. The fabrics were characterized with respect to their morphological as well as mechanical features. The results of this study outline the strength and versatility of spacer fabrics for tissue engineering applications. The properties of the scaffold can be adjusted at multiple levels: the fiber type and material, the design and binding of the cover areas, and the pile yarn geometry (Figure 1). Cutting the fabricated textiles into individual samples without influencing the material properties and whilst maintaining its lateral porosity was shown to be a particular challenge (Figure 2). However, with specific cooling and heat conduction circular samples ranging from 5 to 26 mm could be prepared. The fabricated samples exhibited an overall porosity of 43.4% and a broad pore size distribution peaking at a size of 560 _m (Figure 3A). The porosity is high enough to enable reproducible hydrogel infiltration and to provide su_cient nutrient supply.

Finally, the mechanical characteristics of the hydrogels, the spacer fabric, and the composites were investigated. A collagen biofunctionalized polysaccharide-based hydrogel was applied. The cell biological, microstructural, and rheological properties of the agarose -collagen material system were intensively studied in previous work [22-28]. The material provides excellent stem cell proliferation as well as di_erentiation capacity. In addition, the blend's angiogenic potential was previously described [28,29]. The current study focused on enhancing the bulk mechanical and shape fidelity properties of this highly biofunctional hydrogel system. In this context, the presented results emphasize the advantage of the biohybrid, textile-integrating approach. Fiber-reinforced hydrogel composites exhibited a significantly enhanced compressive modulus compared to their native counter parts. Interestingly, the results further indicate that by combining polysaccharide blending and spacer fabric reinforcement, the mechanics of collagen hydrogels, which are still considered the gold-standard in tissue engineering, can be modulated over two orders of magnitude. Besides the integration of textiles and fibers, in the literature other methods for the mechanical reinforcement of hydrogels are described, such as blending and dual crosslinking of natural and synthetic materials [30], or hybrid bioprinting, where hydrogels are deposited in parallel with biodegradable polymers [29].

While blending and dual crosslinking allows the targeted adjustment of the mechanical properties of hydrogels in the lower elasticity range (e.g., 5 -25 kPa), comparatively sti_ sca_olds can be achieved by hybrid bioprinting (e.g., 30 -50 MPa) [30,31]. In this context, the presented strategy offers certain advantages with respect to its broad adjustability. Using the described fiber-reinforced hydrogel platform a medically relevant range (0.2-100 kPa) can be addressed, which bridges the comparatively elastic hydrogel blends and the rigid scaffolds obtained by hybrid bio printing.

For successful cell proliferation and tissue development, the choice of the 3D knitted fabric is very important regarding the regulatory effects of the cells' microenvironment [32,33]. Following the detailed technical investigation, the metabolic activity, cell number, and adipogenic differentiation of MSCs seeded onto warp-knitted PET fabrics were studied. The ability of the cells to proliferate and differentiate within the 3D environment was examined. It is well known that cell responses may differ in 3D microenvironments compared to 2D conditions [34]. For this reason, PET was selected as prototypic material, which was shown to enable cell adhesion [2]. Two days after seeding the MSCs onto the scaffolds, successful cell attachment to the surface of the 3D-PET-sca_old could be observed using 2-photon microscopy (Figure 1A). Using the presto blue assay, an increased metabolic activity of the cells could be detected in the course of the cultivation period, which indicated proliferation.

Different volumes were pipetted from a stock suspension of 106 cells/mL, to seed the desired cell numbers on the scaffold (50-400 L). Presumably, because the swelling volume of the PET structure at 19.6 mm3 was not sufficient to absorb the complete media during seeding, with increasing cell numbers, the initial PB conversion of 100,000-400,000 cells were all on similar levels. This suggests that in these approaches the same amount of MSCs adhered to the scaffold. However, we did not measure the PB or CV data on the plates after removal of the scaffold, which could have indicated if the cell suspension traversed the PET scaffold, so that cells just passed through it. Notwithstanding, seeding 50,000 cells in a smaller volume of cell suspension reduced the PB data at Day 0. It should be critically assessed that PET material, which is not biodegradable, was applied throughout this study. Thus, it cannot be used as a carrier framework for cells in the in vivo model.

Further research is therefore required to develop an equivalent biodegradable scaffold, e.g., from PCL or PLA filaments, which can be used for future in vivo studies. Nevertheless, the scaffold and the applied materials were shown to be cytocompatible, exhibited increasing metabolic activity of the cells in the course of the experiment, and indicated high proliferation potential and favorable cell viability. After 14 days of culture, the metabolic activity on the scaffolds initially seeded with 50,000 cells reached the same level as the other groups indicating a similar cell count. This hypothesis was supported by the results of the crystal violet assay 28 days after seeding of the cells that showed similar cell numbers for all groups including the control group of 2D seeded cells. From these

results it can be concluded that the PET scaffold had no negative impact on cell proliferation or viability in comparison to a regular 2D culture. The results of the measurements show that there seems to be saturation of the 3D knitted fabric, where an increase in the number of cells cannot be reached after 28 days at the latest. In summary, the construct offered optimal conditions for allowing the cells to proliferate over this period of 28 days.

Previous studies have usually used a high cell count for seeding onto scaffolds. Thus, just a limited statement about the proliferation on tissues was possible [35-39]. We now showed with different numbers of cells how development of proliferation progresses and a saturation of the 3D knitted fabric is achieved.

In addition, it has been possible to induce the differentiation of the MSCs into the adipogenic line.

We were able to prove the differentiation by an oil red staining and additionally adipokines analyses by ELISA. It has been possible to identify an optimal three-dimensional framework for proliferation and differentiation of MSCs, which in a further step will be transferred into a biodegradable material.

Conclusion

To sum up, the developed spacer fabric was shown to be a promising platform technology to biofabricate textile-reinforced hydrogel structures with pronounced and tunable mechanical, morphological, as well as biological features. In the future, this platform technology can be applied for a broad range of tissue engineering applications, including load bearing tissues (cartilage or bone) for regenerative medicine as well as soft tissues for reconstructive surgery.

References

1. Caplan AI (1991) Mesenchymal stem cells. J Orthop Res 9: 641-650.
2. Dominici M, Le Blanc K, Mueller I, Slaper-Cortenbach I, Marini FC, et al. (2006) Minimal criteria for defining multipotent mesenchymal stromal cells. The International Society for Cellular Therapy position statement. Cytotherapy 8: 315-317.
3. Park S, Choi Y, Jung N, Yu Y, Ryu KH, et al. (2016) Myogenic differentiation potential of human tonsil-derived mesenchymal stem cells and their potential for use to promote skeletal muscle regeneration. Int J Mol Med 37: 1209-1220.
4. Prockop DJ, Zuk PA, (2001) Stem cell research has only just begun. Science 293: 211-212.
5. D'Andrea F, Francesco FD, Ferraro GA, Desiderio V, Tirino V, et al. (2008) Large-scale production of human adipose tissue from stem cells: A new tool for regenerative medicine and tissue banking. Tissue Eng. Part C Methods 14: 233-242.
6. Beier JP, Horch RE, Bach AD, (2009) Breast reconstruction after breast-cancer surgery. N. Engl J Med 360: 418-419.
7. Ludolph I, Arqudas A, Schmitz M, Boos AM, Taeger CD, (2016) Cracking the perfusion code?: Laser-assisted Indocyanine Green angiography and combined laser Dopplerspectrophotometry for intraoperative evaluation of tissue perfusion in autologous breast reconstruction with DIEP or ms-TRAM flaps. J. Plast. Reconstr. Aesthet. Surg 69: 1382-1388.
8. Ludolph I, Horch R.E, Harlander M, Arqudas A, Bach A.D, et al. (2015) Is there a rationale for autologous breast reconstruction in older patients? A retrospective single center analysis of quality of life, complications and comorbidities after DIEP or ms-TRAM Flap using the BREAST-Q. Breast J 21: 588-595.
9. Sicari BM, Rubin JP, Dearth CL, Wolf MT, Ambrosio F, et al. (2014) An acellular biologic scaffold promotes skeletal muscle formation in mice and humans with volumetric muscle loss. Sci. Transl. Med 6: 234-258.
10. Pollot BE, Corona BT, (2016) Volumetric Muscle Loss. In Skeletal Muscle Regeneration in the Mouse: Methods and Protocols, 1st ed.; Kyba, M., Ed.; Springer: New York, NY, USA 20: 19-31.
11. Dong R, Ma PX, Guo B, (2020) Conductive biomaterials for muscle tissue engineering. Biomaterials 229: 119584.
12. Murugan R, Ramakrishna S, (2017) Design strategies of tissue engineering sca_olds with controlled fiberorientation. Tissue Eng 13: 1845-1866.
13. Komlev VS, Popov VK, Mironov AV, Fedotov AY, Teterina AY et al. (2015) 3D printing of octacalcium phosphate bone substitutes. Front. Bioeng. Biotechnol 3: 81.
14. Huber A, Pickett A, Shakeshe KM (2007) Reconstruction of spatially orientated myotubes in vitro using electrospun, parallel microfibre arrays. Eur. Cell Mater 14: 56-63.
15. Zhao W, Ju YM, Christ G, Atala A, Yoo JJ, et al. (2013) Diaphragmatic muscle reconstruction with an aligned electrospun poly ("-caprolactone)/collagen hybrid sca_old. Biomaterials 34: 8235 -8240.
16. Huang G, Li F, Zhao X, Ma Y, Li Y, et al. (2017) Functional and biomimetic materials for engineering of the three-dimensional cell microenvironment. Chem. Rev 117: 12764-12850.
17. Ma Y, Lin M, Huang G, Li Y, Wang S, et al. (2018) 3D spatiotemporal mechanical microenvironment: A Hydrogel-Based Platform for Guiding Stem Cell Fate. Adv Mater 30: 1705911.
18. Koch S, Flanagan TC, Sachweh JS, Tanios F, Schnoering H, et al. (2010) Fibrin-polylactide-based tissue-engineered vascular graft in the arterial circulation. Biomaterials 31: 4731 -4739.
19. Weber M, Heta E, Moreira R, Gesche VN, Schermer T, et al. (2014) Tissue-engineered fibrin-based heart valve with a tubular leaflet design. Tissue Eng. Part C Methods 20: 265 -275.
20. Ruhl T, Storti G, Pallua N. (2018) Proliferation, Metabolic activity, and adipogenic di_erentiation of human preadipocytes exposed to 2 surfactants in vitro. J. Pharm. Sci 107: 1408 -1415.
21. Gillies RJ, Didier N, Denton M. (1986) Determination of cell number in monolayer cultures. Anal. Biochem 159: 109-113.
22. Sonnaert M, Papantoniou I, Luyten FP, Schrooten JI. (2015) Quantitative validation of the presto blue metabolic assay for online monitoring of cell proliferation in a 3D perfusion bioreactor system. Tissue Eng. Part C Methods 21: 519-529.
23. Zuk PA, Zhu M, Mizuno H, Huang J, Futrell JW, et al. (2001) Multilineage cells from human adipose tissue: Implications for cell-based therapies. Tissue Eng 7: 211 -228.
24. Duarte Campos DF, Blaeser A, Korsten A, Neuss S, Jäkel J, et al. (2015) The sti_ness and structure of three-dimensional printed hydrogels direct the di_erentiation of mesenchymal stromal cells toward adipogenic and osteogenic lineages.

Tissue Eng. Part A 21: 740-756.
25. Köpf M, Campos DF, Blaeser A, Sen KS, Fischer H, (2016) A tailored three-dimensionally printable agarose-collagen blend allows encapsulation, spreading, and attachment of human umbilical artery smooth muscle cells. Biofrabrication 8: 025011.
26. Forget A, Blaeser A, Miessmer F, Köpf M, Campos DFD, et al. (2017) Mechanically tunable bioink for 3D bioprinting of human cells. Adv. Healthc. Mater 6: 1700255.
27. Blaeser A, Duarte Campos DF, Puster U, Richtering W, Stevens MM, et al. (2016) Controlling shear stress in 3D bioprinting is a key factor to balance printing resolution and stem cell integrity. Adv. Healthc.Mater 5: 326-333.
28. Duarte Campos DF, Blaeser A, Buellesbach K, Sen KS, XunW, et al. (2016) Bioprinting organotypic hydrogels with improved mesenchymal stem cell remodeling and mineralization properties for bone tissue engineering. Adv. Healthc. Mater 5: 1336-1345.
29. Kreimendahl F, Köpf M, Thiebes AL, Duarte Campos DF, Blaeser A, et al. (2017) Three-dimensional printing and angiogenesis: Tailored agarose-type I collagen blends comprise three-dimensional printability and angiogenesis potential for tissue-engineered substitutes. Tissue Eng. Part C Methods 23: 604-615.
30. Duarte Campos DF, Bonnin Marquez A, O'Seanain C, Fischer H, Blaeser A, et al. (2019) Exploring cancer cell behavior in vitro in three-dimensional multicellular bioprintable collagen-based hydrogels. Cancers (Basel) 11: 180.
31. Ma Y, Ji Y, Zhong T, WanW, Yang Q, et al. (2017) Bioprinting-based PDLSC-ECM screening for in vivo repair of alveolar bone defect using cell-laden, injectable and photocrosslinkable hydrogels. ACS Biomater. Sci. Eng 3: 3534-3545.
32. Kang HW, Lee SJ, Ko IK, Kengla C, Yoo JJ, et al. (2016) A 3D bioprinting system to produce human-scale tissue constructs with structural integrity. Nat. Biotechnol 34: 312-319.
33. Kang HW, Lee SJ, Ko IK, Kengla C, Yoo JJ, et al. (2016) Printing human-scale tissues in three dimension. Nat. Biotechnol 13: 289.
34. Cukierman E, Pankov R, Yamada KM, (2002) Cell interactions with three-dimensional matrices. Curr. Opin. Cell Biol 14: 633-640.
35. Meinel L, Hofmann S, Karageorgiou V, Zichner L, Langer R, et al. (2004) Engineering cartilage-like tissue using human mesenchymal stem cells and silk protein sca_olds. Biotechnol. Bioeng 88: 379-391.
36. Patel DK, Lim KT, (2019) Biomimetic Polymer-based engineered scaffolds for improved stem cell function. Materials (Basel) 12: 2950.
37. Neves AA, Medcalf Z, Brindle KM, (2005) Influence of stirring-induced mixing on cell proliferation and extracellular matrix deposition in meniscal cartilage constructs based on polyethylene terephthalate scaffolds. Biomaterials 26: 4828-4836.
38. Bjerre L, Bünger CE, Kassem M, Mygind T, (2008) Flow perfusion culture of human mesenchymal stem cells on silicate-substituted tricalcium phosphate scaffolds. Biomaterials 29: 2616-2627.
39. Benedikt S, Caroline E, Nikola G, Tim R, Astrid S O, et al (2020) Materials 13: 3518